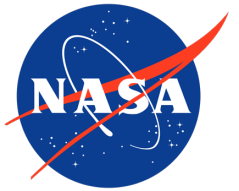

Anisotropic Mach Cone Aligned Mesh Adaptation for Low Boom Simulations

Chase Ashby, Jeffrey Housman, Jared Duensing
Computational Aerosciences Branch
NASA Ames Research Center

AIAA Aviation Forum, June 12th – June 16th , 2023

Outline

- Introduction
  - Motivation and Objectives
  - Low-Boom Simulations
- Methodology
  - Overset Grid System
  - Adaptation Equations
  - Error Indicator Formulations
- Results
  - X-59 C608 Demonstrator Model
- Summary

Motivation

- Evaluation of low boom aircraft designs rely on accurate predictions of ground-level noise
- The Launch, Ascent, and Vehicle Aerodynamics (LAVA) framework uses a three-step prediction procedure
- Near-field CFD simulations demand the majority of the required computational resources

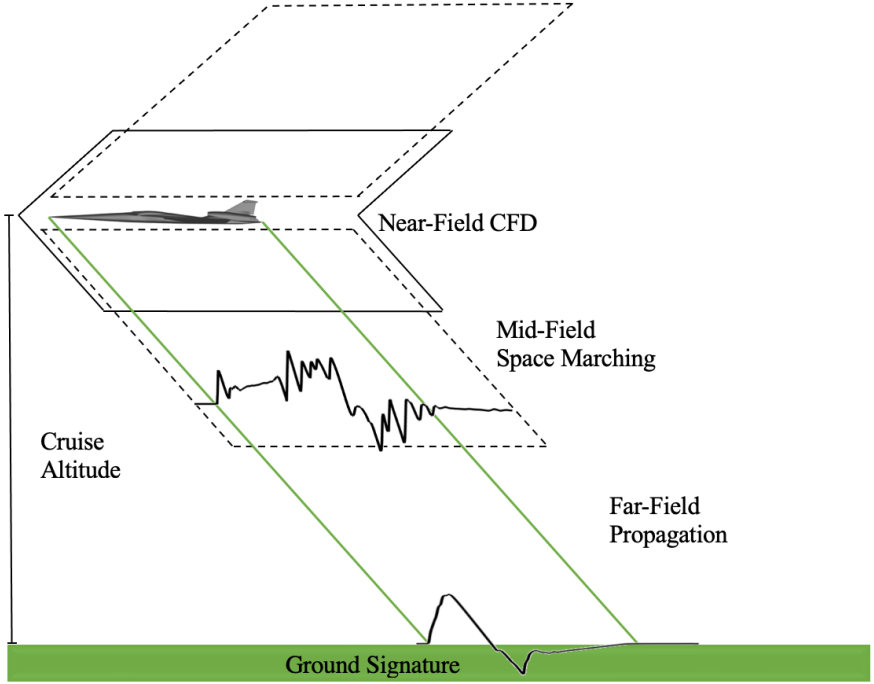

Low Boom Simulation Procedure

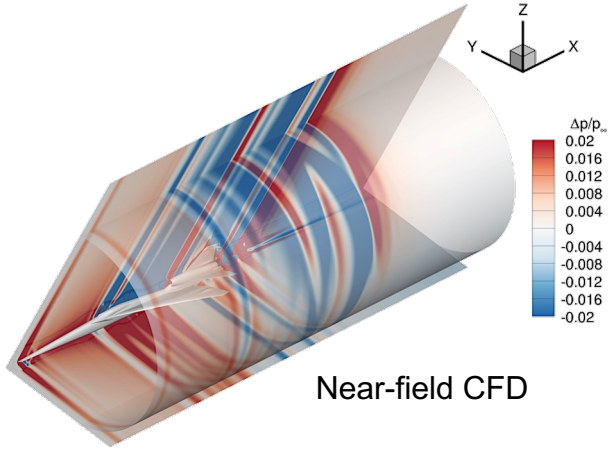

Near-field CFD

Interpolation
+
Space Marching

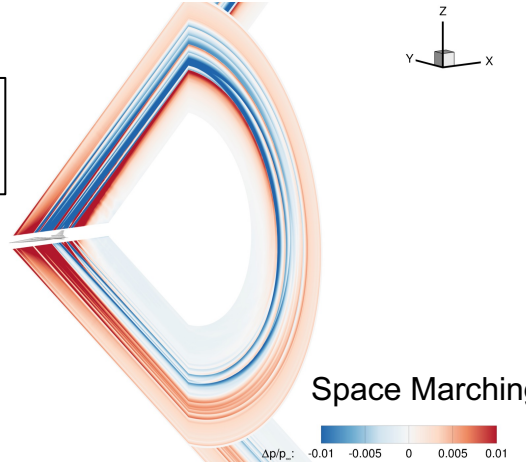

Space Marching

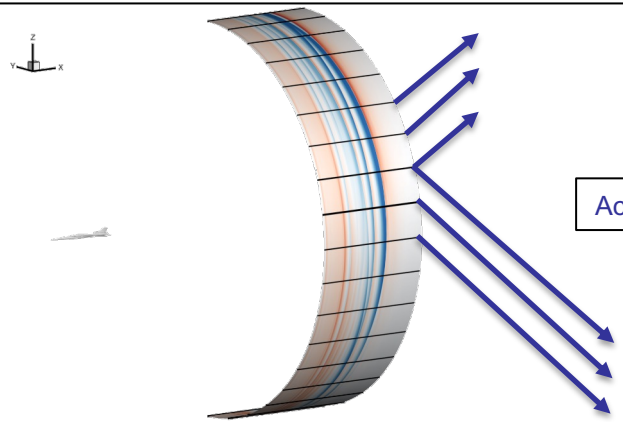

Pressure Cylinder Extraction

Acoustic Propagation

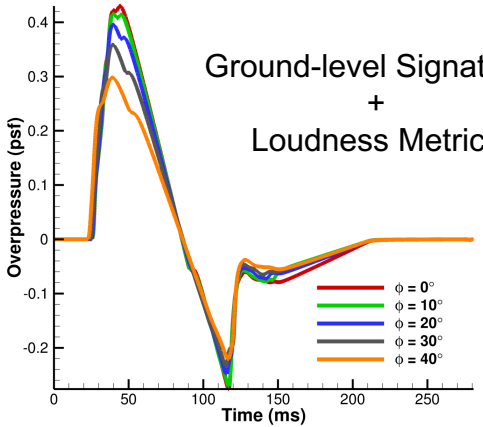

Ground-level Signatures
+
Loudness Metrics

Objectives

1. Automate the off-body grid generation procedure for near-field simulations
   - Increase robustness to flight plan changes

2. Generate improved CFD grid system with fixed degrees of freedom
   - Reduce resource requirements for achievable accuracy levels

3. Construct error indicators to facilitate rapid anisotropic mesh adaptation
   - Capture error for non-symmetric complex supersonic flows

Methodology: Overset Grid System

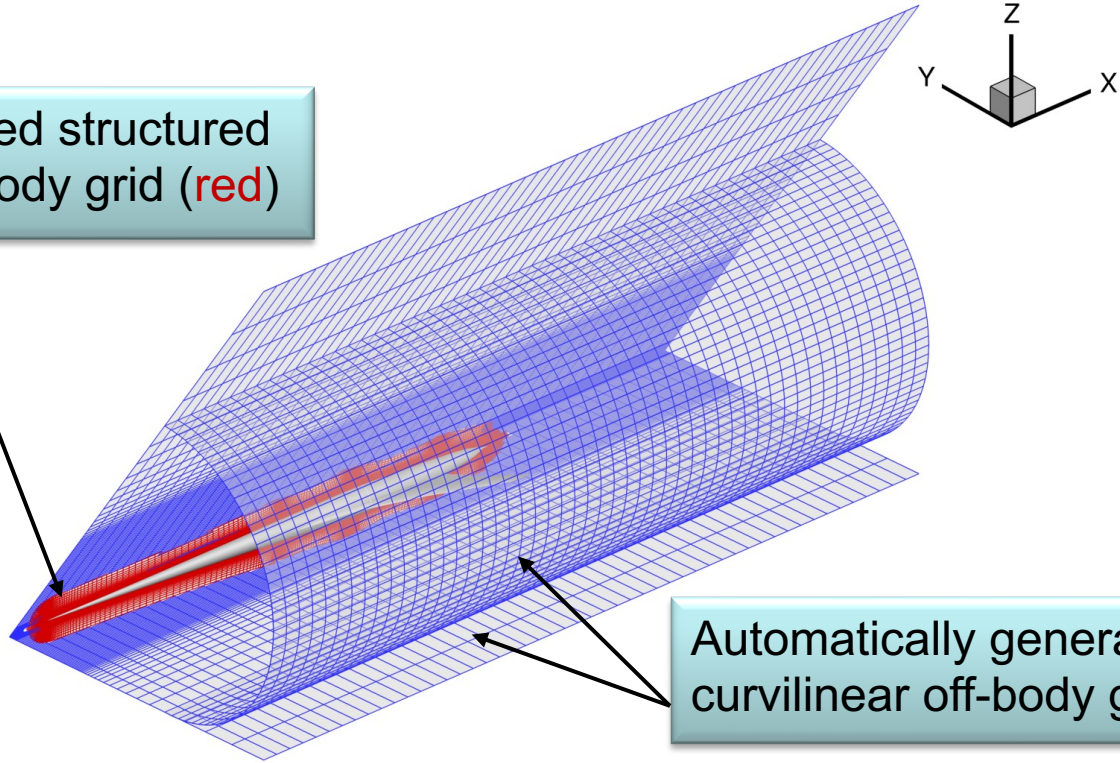

Manually generated structured curvilinear near-body grid (red)

Automatically generated structured curvilinear off-body grid (blue)

Methodology

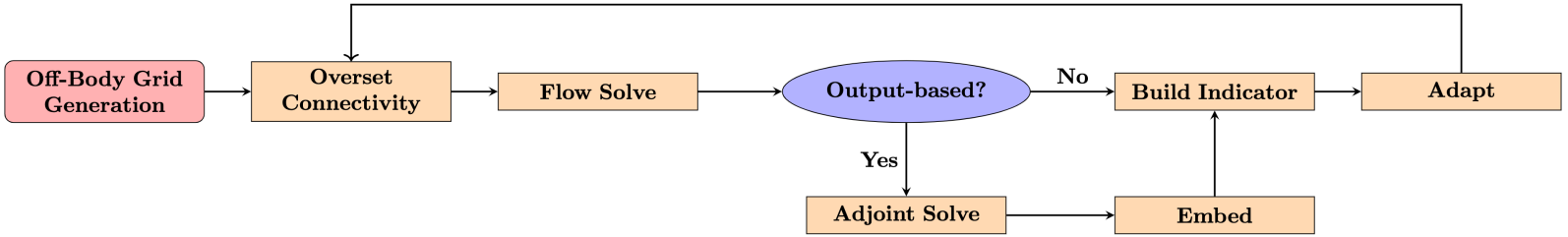

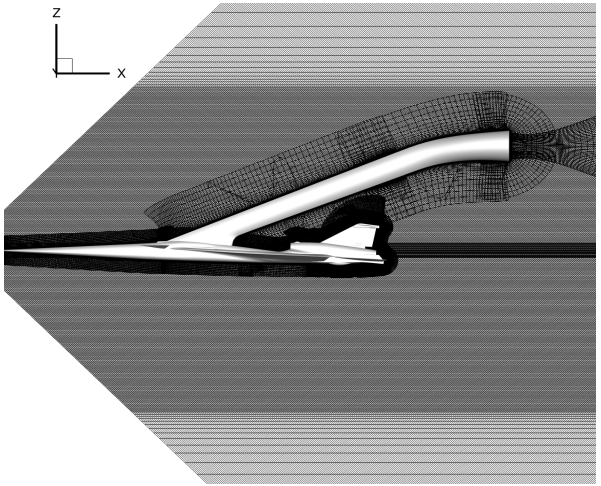

Initial Off-body

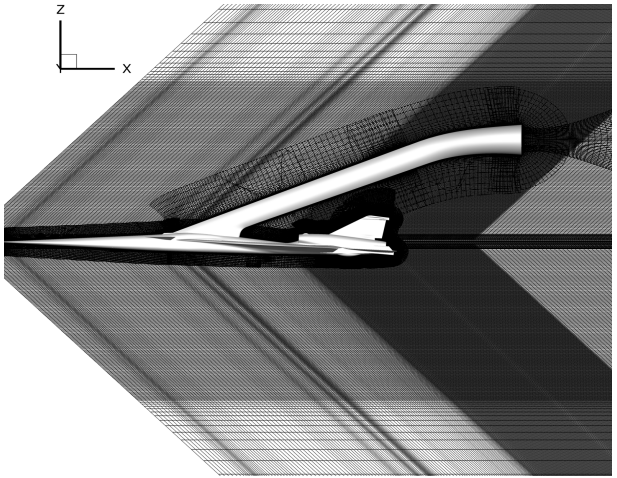

Adapted Off-body

Methodology: Adaptation Equations

- Direction-based mesh redistribution is governed by the equation

$$w_i \underbrace{\Delta s_i}_{\text{cell-size}} = C$$

Discrete equidistribution principle

- Adaptation weights control the location of local refinement

$$w_i = 1 + A \underbrace{f_i}_{\text{error indicator}}$$

- Clustering constant limits the maximum and minimum cell-size

$$A = \underbrace{c_{\mathrm{f}} r_{\mathrm{f}}}_{\text{coarsening and refinement factors}} \frac{\Delta s^0_{\max}}{\Delta s^0_{\min}} - 1$$

Methodology: Error Indicators

- The construction of direction-based indicators relies on the initial computation of standard error indicators

- **Feature-based** indicators target errors in a specific flow quantity
  - Mach, vorticity, pressure disturbance, etc.

- **Output-based** indicators target errors in a single or multiple scalar output quantities of interest
  - Lift, drag, pitching moment, line integral of pressure, etc.

Methodology: Error Indicators

- Feature-based indicators are formed from the second undivided difference

$$e_i = |q_{i+1} - 2\,q_i + q_{i-1}|$$

- This is proportional to the remaining error term of linear interpolation across cell i

$$e_i \propto \frac{(\Delta\xi)^2}{8} \max_{\xi_i \le \xi \le \xi_{i+1}} |q''(\xi)|$$

- Normalize by a reference quantity and compute the maximum over each computational space direction

$$e(\xi_j, \eta_k, \zeta_l) = \max_{i=j,k,l} \frac{|q_{i+1} - 2q_i + q_{i-1}|}{q_{\text{ref}}}$$

Methodology: Error Indicators

- Near-field CFD governed by RANS in strong conservative form

$$\mathbf{R}(\mathbf{Q}) = 0 \text{ in } \Omega$$

- Output-based indicators target the coarse grid functional discretization error

$$\varepsilon = \left| J(\mathbf{Q}) - J_{\mathrm{H}}(\mathbf{Q}_{\mathrm{H}}) \right|$$

Methodology: Error Indicators

- Discrete adjoint derivation gives the estimate

$$J(\mathbf{Q}) - J_{\mathrm{H}}(\mathbf{Q}_{\mathrm{H}}) \approx \frac{r_{\mathrm{f}}^{p}}{r_{\mathrm{f}}^{p}-1}\left(J_{\mathrm{h}}(\mathbf{Q}_{\mathrm{h}}^{\mathrm{LO}}) - J_{\mathrm{H}}(\mathbf{Q}_{\mathrm{H}})\right) - \frac{r_{\mathrm{f}}^{p}}{r_{\mathrm{f}}^{p}-1}\left[\left(\boldsymbol{\psi}_{\mathrm{h}}^{\mathrm{LO}}\right)^{T}\mathbf{R}_{\mathrm{h}}(\mathbf{Q}_{\mathrm{h}}^{\mathrm{LO}}) + (\boldsymbol{\psi}_{\mathrm{h}}^{\mathrm{HI}} - \boldsymbol{\psi}_{\mathrm{h}}^{\mathrm{LO}})^{T}\mathbf{R}_{\mathrm{h}}(\mathbf{Q}_{\mathrm{h}}^{\mathrm{LO}})\right]$$

- High- and low-order prolongation operators are defined

$$\mathbf{Q}_{\mathrm{h}}^{\mathrm{LO}} = \mathbf{P}_{\mathrm{LO}}\mathbf{Q}_{\mathrm{H}}$$
$$\boldsymbol{\psi}_{\mathrm{h}}^{\mathrm{LO}} = \mathbf{P}_{\mathrm{LO}}\boldsymbol{\psi}_{\mathrm{H}}$$

Methodology: Error Indicators

- Output-based indicator on the embedded grid

$$e_{\mathrm{h}} = \left(\boldsymbol{\psi}_{\mathrm{h}}^{\mathrm{HI}} - \boldsymbol{\psi}_{\mathrm{h}}^{\mathrm{LO}}\right)^{T} \mathbf{R}_{\mathrm{h}}(\mathbf{Q}_{\mathrm{h}}^{\mathrm{LO}})$$

- Output indicator is defined

$$J(\mathbf{Q}) := \sum_{i=1}^{N_{\mathrm{fringe}}} \left(\frac{\Delta p_i}{p_\infty}\right)^2$$

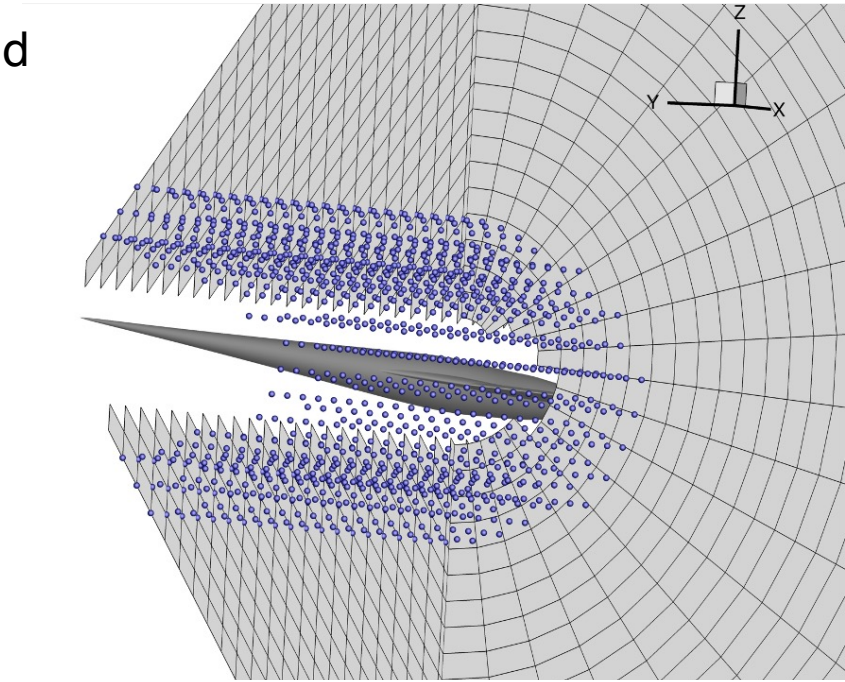

Space Marching Fringe Points

Methodology: Error Indicators

- For a fixed radial surface ζ^* a streamwise indicator is computed

$$g(\xi) = \max_{\eta} |e_0(\xi, \eta, \zeta^*)|$$

- Apply a low number of elliptic smoothing iterations

$$g_i^{\mathrm{s}} = \frac{g_{i-1} + 4g_i + g_{i+1}}{6}$$

- Smoothed indicator is mapped between [0,1)

$$f(\xi, \eta; \zeta^*) = \tanh(\beta\, g^{\mathrm{s}}(\xi)) \in [0, 1)$$

$$\beta = \tanh^{-1}(0.8)/(C\,\bar{g})$$

Methodology: Error Indicators

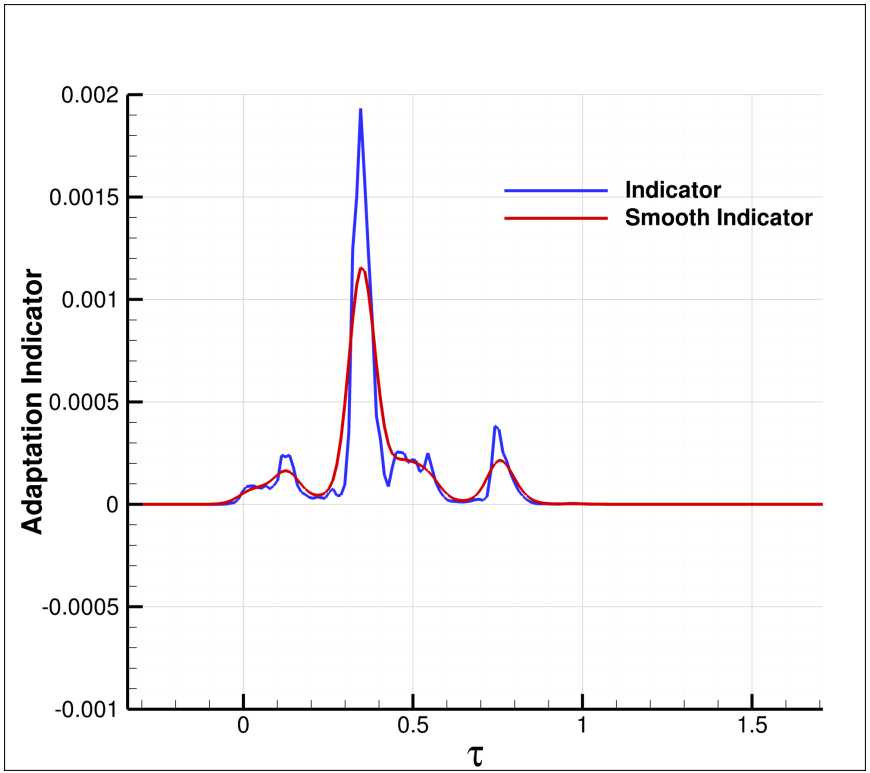

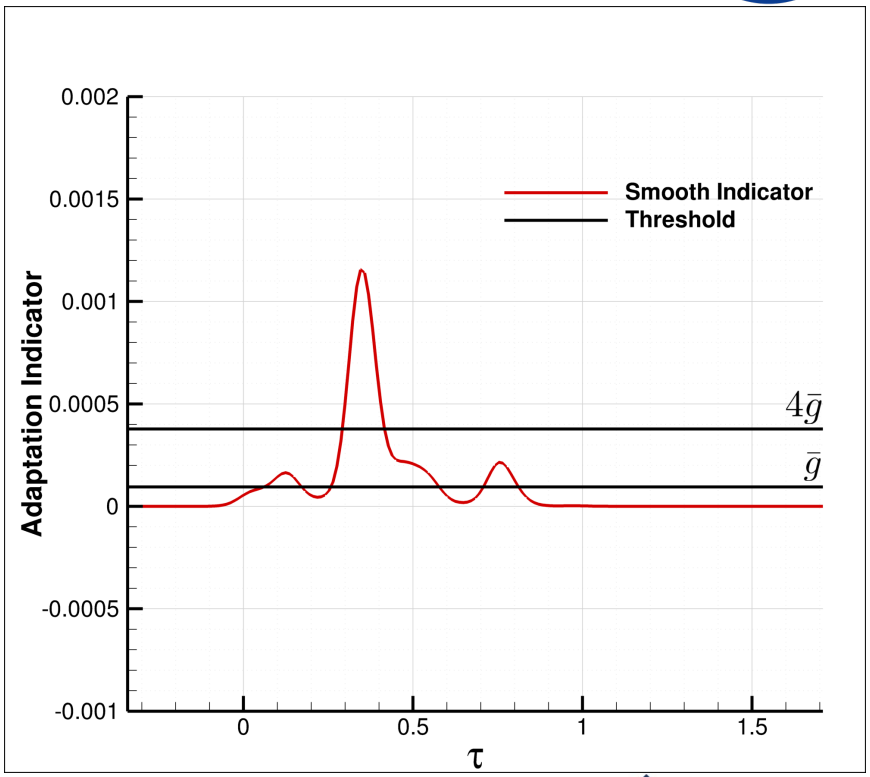

Methodology: Error Indicators

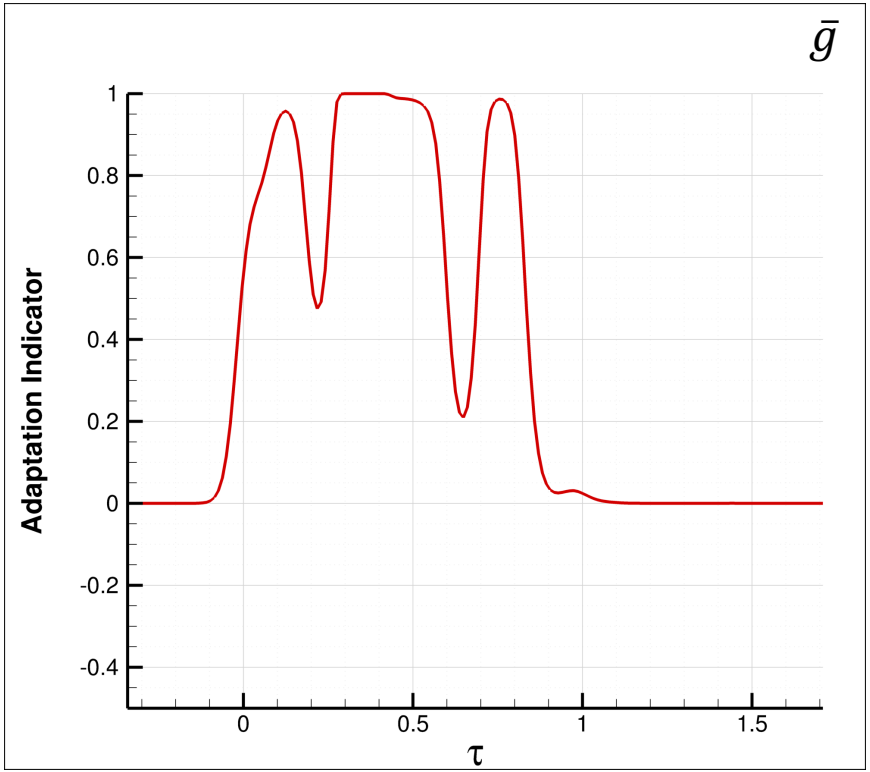

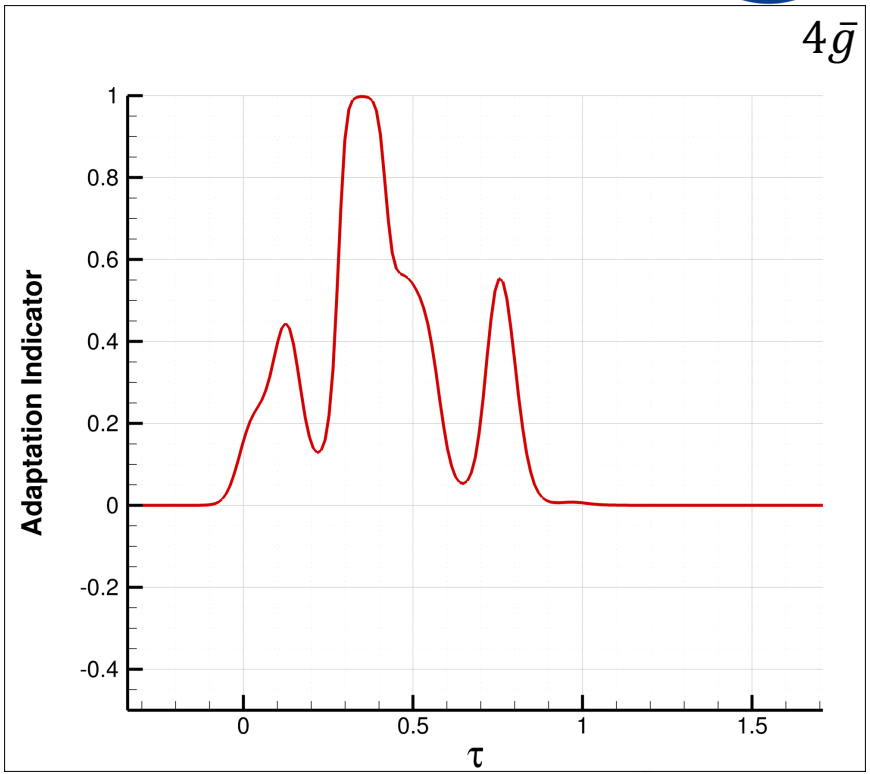

Methodology: Error Indicators

- Direction-based surface indicator is interpolated to off-body grid using a normalized distance metric

$$\tau = \frac{x - r\sqrt{M_\infty^2 - 1}}{L_{\text{body}}}$$

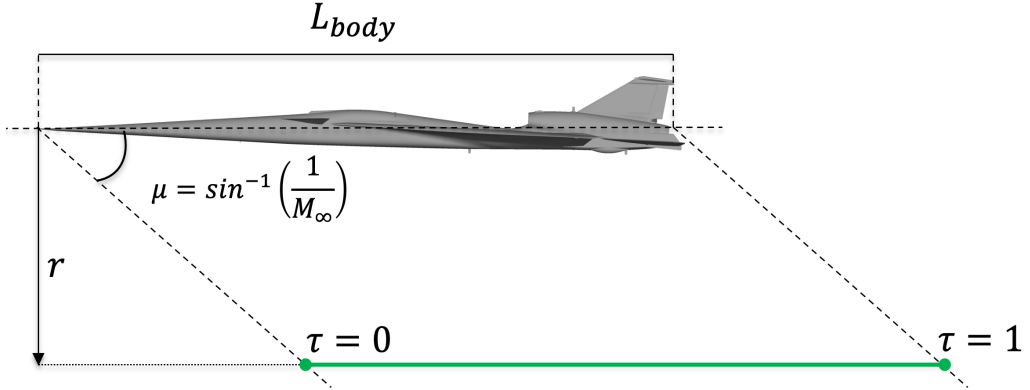

Methodology: Error Indicators

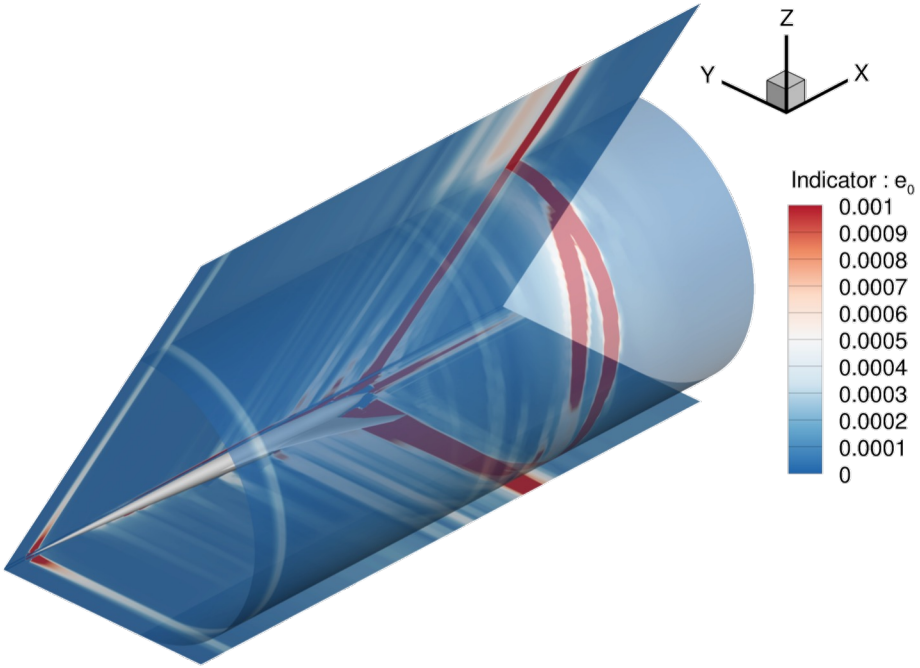

Initial Feature-Based Error Indicator

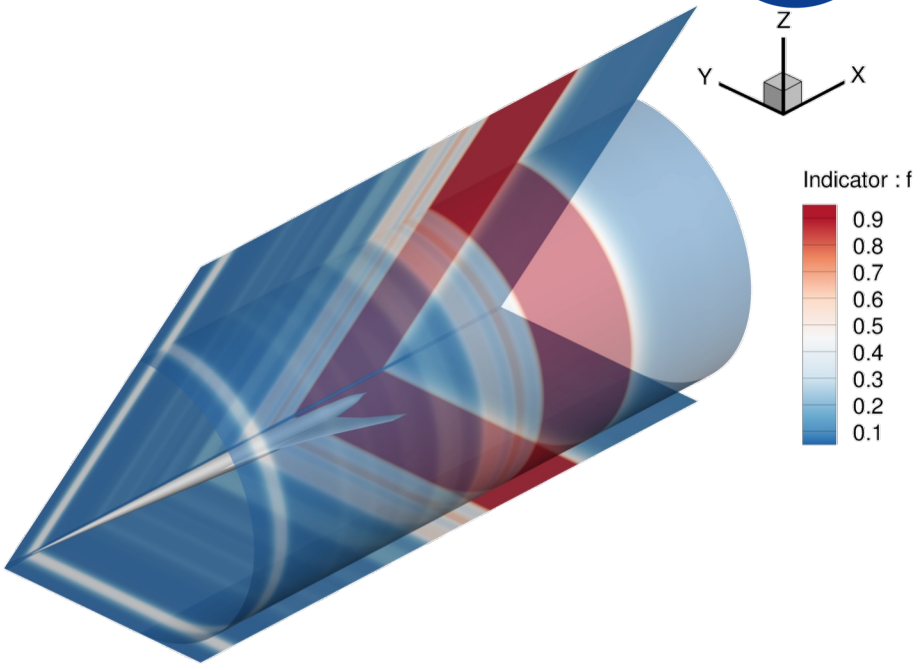

Final Direction-based Error Indicator

Methodology: Error Indicators

- Direction-based indicator construction procedure is generalizable
- Adaptation equations are solved along **ONE** coordinate line
  - Resulting coordinate displacements are used to update the rest of the off-body grid
- Sequential multi-directional adaptation
  - Studied combined circumferential and streamwise adaptation
  - No benefit of circumferential adaptation has been observed

Results

- Streamwise adapted off-body grids are compared to automatically generated uniform grids
  - Constant streamwise and circumferential spacing
- Near-body grids are held fixed
  - Grid refinement studies performed during AIAA SBPW
- Comparison of off-body grid-levels for feature-based and output-based indicators
  - 1st order adjoint solver used for presented results

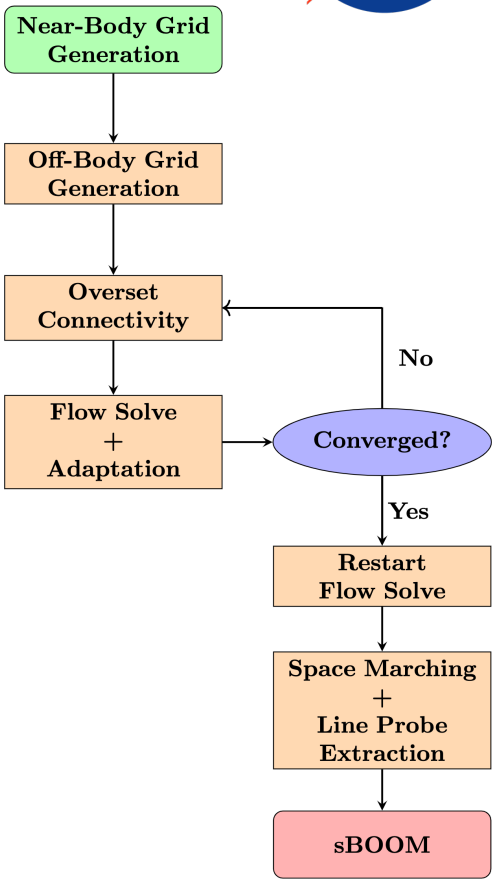

Results: Benchmark

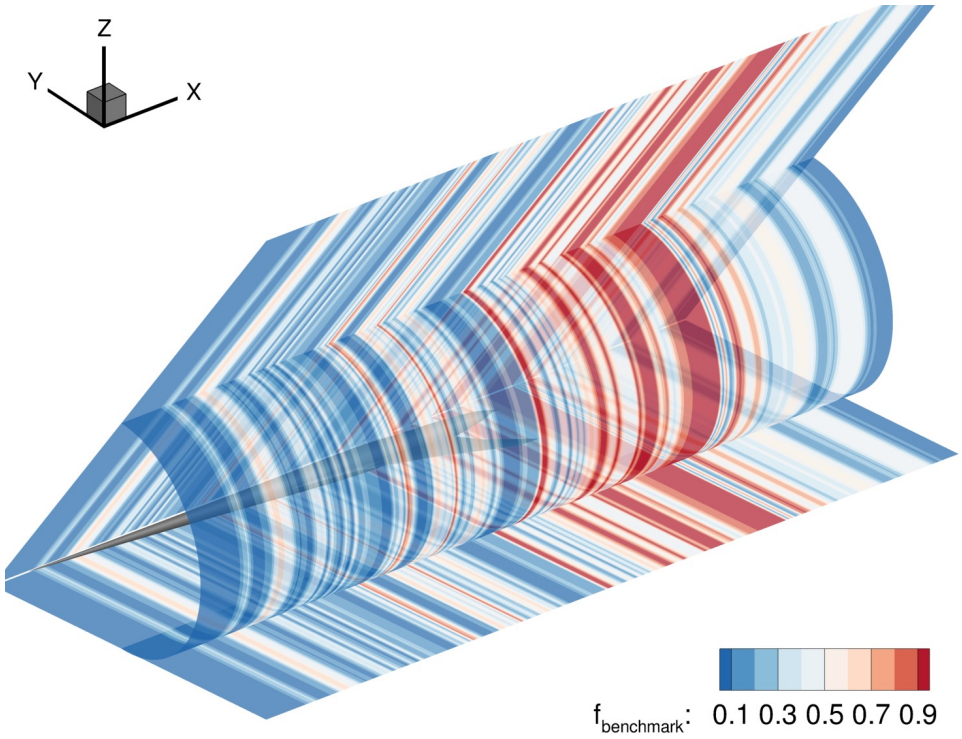

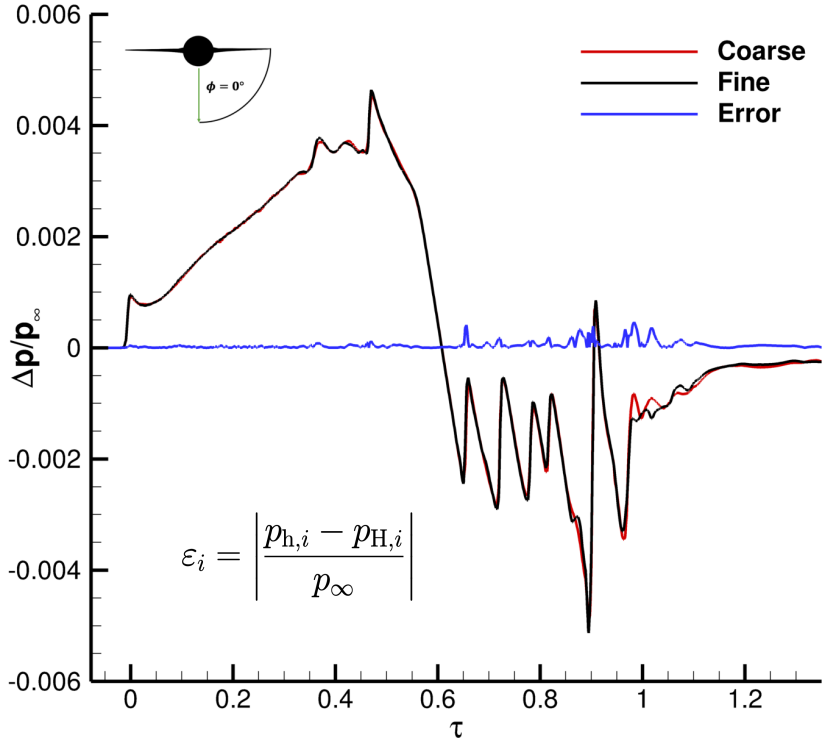

Benchmark Direction-Based Indicator

Results: X-59 C608

Reference length : $L_{ref} = 27.432\ m$

Cruise Altitude : 16,215 m

Mach = 1.4, Re/m = 4.3 million, and $\alpha = 2.15^{\circ}$

Front View

Side View

Results: X-59 C608

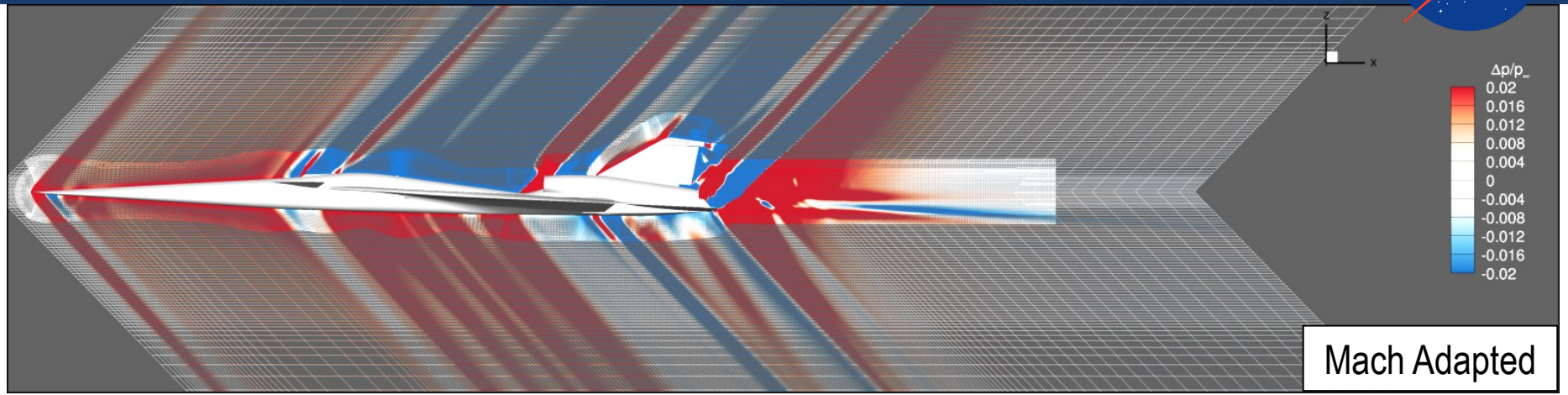

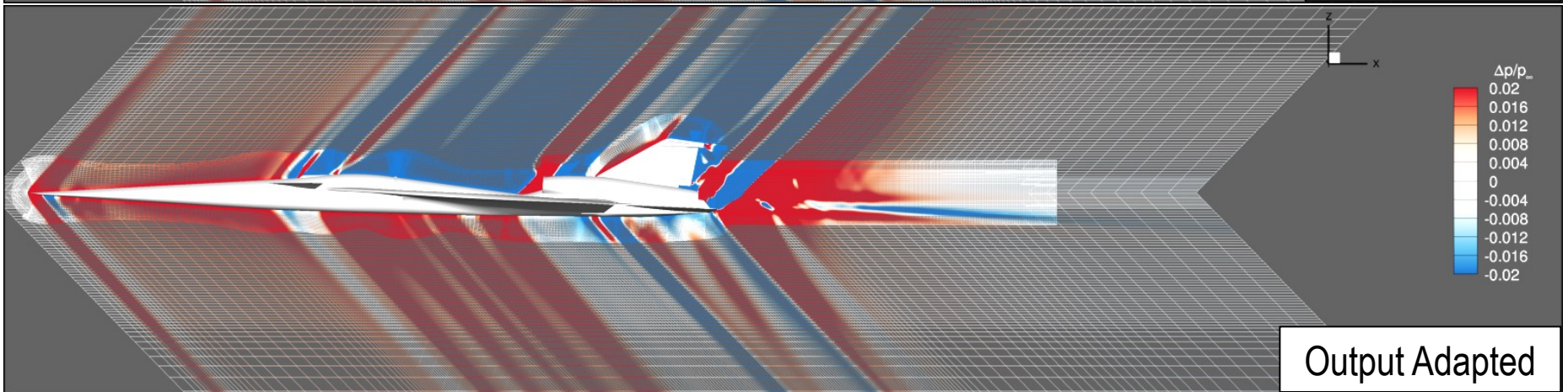

Near-field Accuracy Improvement

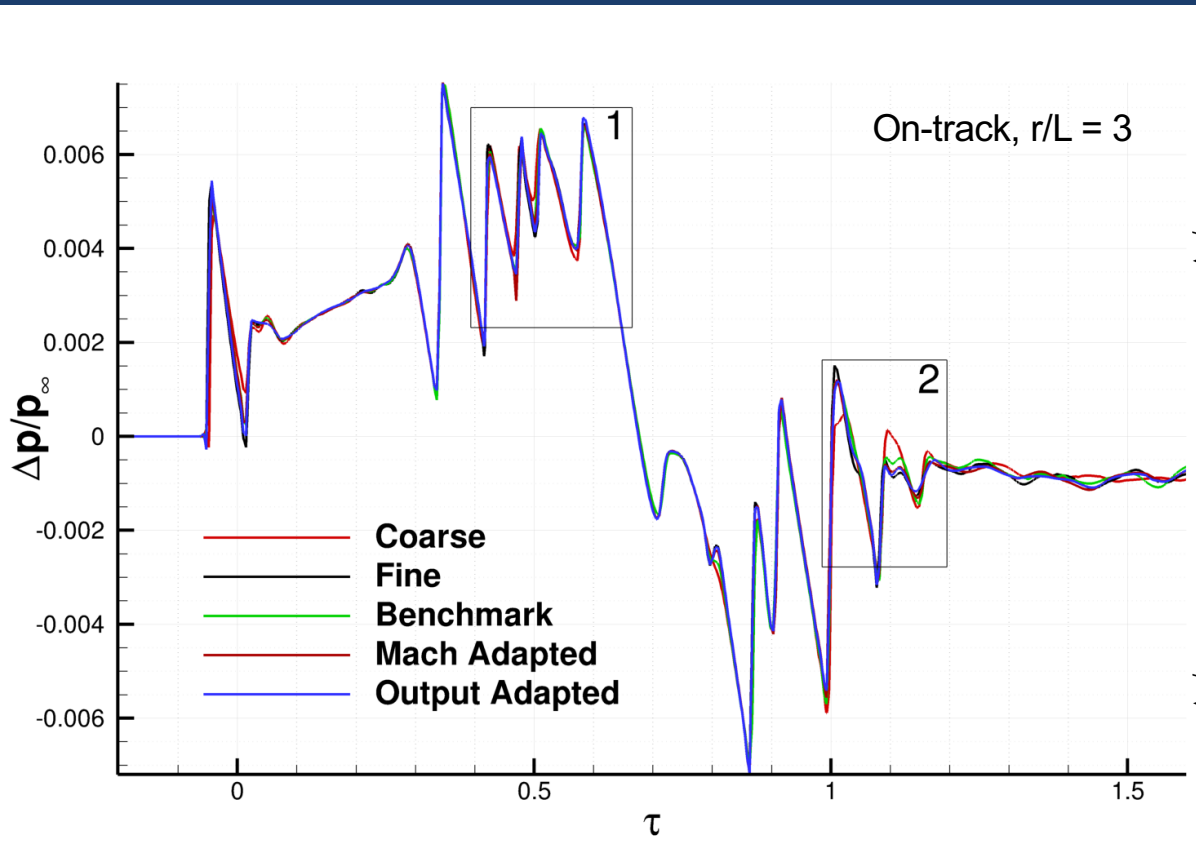

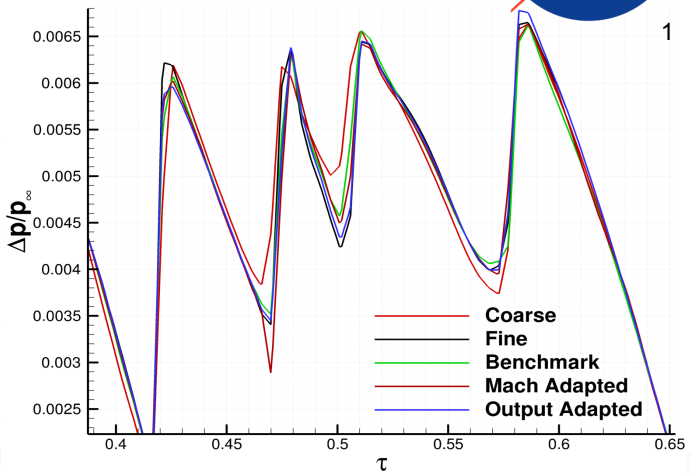

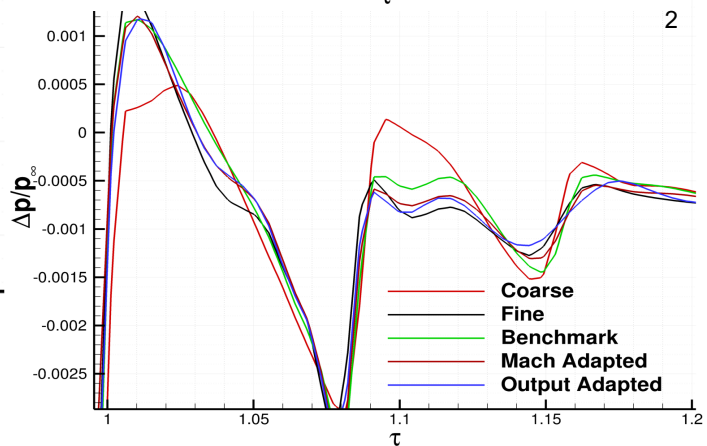

Near-Field Propagation Difference

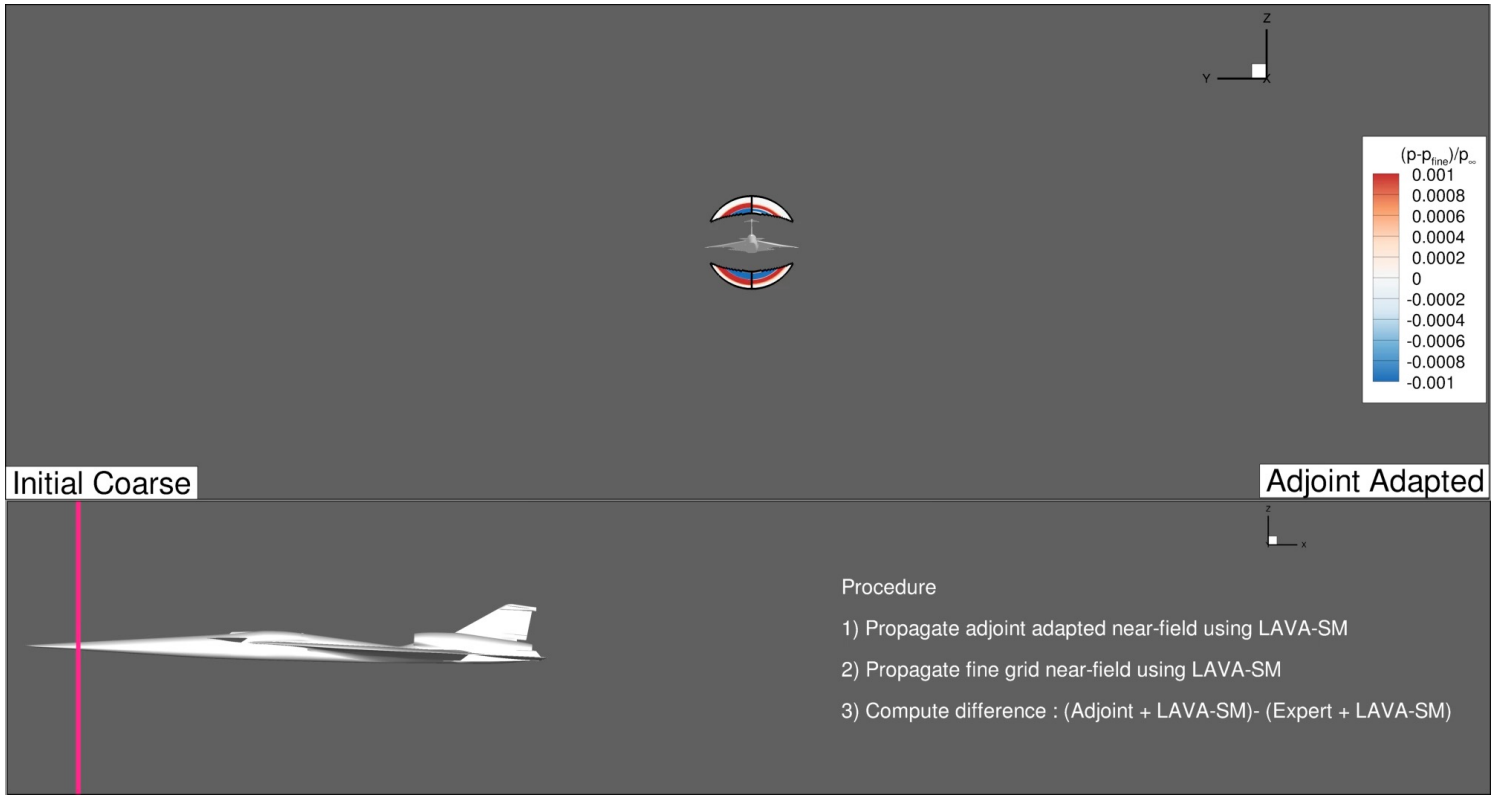

Ground Level Accuracy Improvement

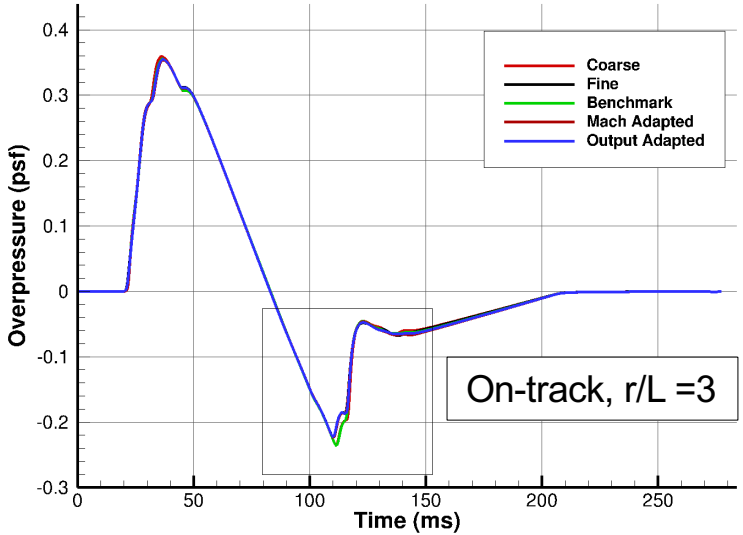

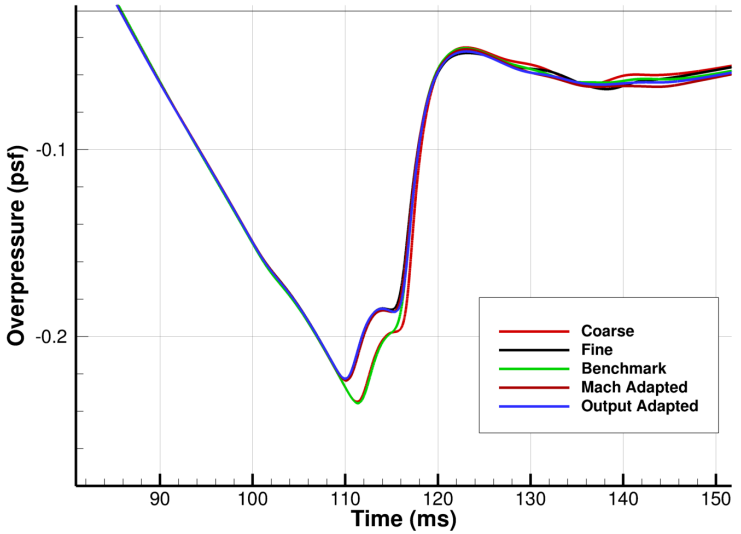

Grid	ASEL [dB(A)]	BSEL [dB]	CSEL [dB(C)]	PL [dB]	ASEL Rel. Error	BSEL Rel. Error	CSEL Rel. Error	PL Rel. Error
Fine	62.21	76.49	91.27	76.53				
Coarse	63.40	77.78	91.72	77.80	1.917%	1.692%	0.497%	1.660%
Benchmark	62.80	77.22	91.53	77.41	0.946%	0.952%	0.285%	1.149%
Mach Adapted	62.63	76.73	91.29	76.94	0.664%	0.312%	**0.025%**	0.544%
Output Adapted	62.11	76.53	91.30	76.45	**0.160%**	**0.056%**	0.032%	**0.103%**

Cost Analysis

- Off-body grids may not account for the majority of the the total degrees of freedom
  - C608 off-body grid accounts for only 23.59% of total coarse grid nodes
- Off-body grid adaptation procedure cost is compared to LAVA's baseline best practice grid from the 3rd AIAA Sonic Boom Prediction Workshop
- Reference grid has manually generated off-body refinement regions

Cost Analysis

Grid	Total Nodes*	Degrees of Freedom*	Nodes per Core
Reference	161.990	127.379	318,448
Fine	36.329	23.613	295,166
Coarse	29.754	20.874	260,925

*In millions.

3.7x reduction in computational resources

Grid	Connectivity	Primal Solve	Adjoint Solve	Embedding	Adaptation	Restart	**Total**	SBU
Reference	-	1.4	-	-	-	-	1.4	**18.3**
Coarse	0.02	1.59	-	-	-	-	1.77	**4.6**
Fine	0.02	2.60	-	-	-	-	2.62	**6.7**
Benchmark Adapted	0.04	1.59	-	-	-	0.14	1.77	**4.6**
Mach Adapted	0.04	1.59	-	-	-	0.14	1.77	**4.6**
Output Adapted	0.04	1.59	0.10	0.01	0.01	0.14	1.89	**4.9**

Cost Analysis

Grid	ASEL [dB(A)]	BSEL [dB]	CSEL [dB(C)]	PL [dB]	ΔASEL	ΔBSEL	ΔCSEL	ΔPL
Reference	61.59	76.73	91.20	76.81	-	-	-	-
Fine	62.21	76.49	91.27	76.53	1.017%	0.309%	0.076%	0.368%
Coarse	63.40	77.78	91.72	77.80	2.953%	1.378%	0.574%	1.286%
Benchmark	62.80	77.22	91.53	77.41	1.972%	0.640%	0.361%	0.777%
Mach Adapted	62.63	76.73	91.29	76.94	1.687%	**0.002%**	**0.101%**	**0.174%**
Output Adapted	62.11	76.53	91.30	76.45	**0.855%**	0.254%	0.108%	0.470%

On-track loudness metrics propagated from r/L = 3

Grid	ASEL [dB(A)]	BSEL [dB]	CSEL [dB(C)]	PL [dB]	ΔASEL	ΔBSEL	ΔCSEL	ΔPL
Reference	59.09	75.64	89.98	74.42	-	-	-	-
Fine	60.14	75.51	89.90	74.51	1.782%	0.186%	0.086%	0.122%
Coarse	61.80	76.34	90.29	76.24	4.584%	0.928%	0.346%	2.447%
Benchmark	60.91	76.18	90.22	75.58	3.092%	0.718%	0.277%	1.570%
Mach Adapted	60.85	75.90	89.99	75.25	2.982%	0.341%	**0.017%**	1.117%
Output Adapted	60.73	75.77	89.95	75.09	**2.772%**	**0.173%**	0.029%	**0.906%**

Off-track loudness metrics propagated from r/L = 3

Summary

- Introduced a new anisotropic mesh adaptation algorithm for structured curvilinear Mach cone aligned grids
  - Eliminates need for manual off-body grid generation
- Novel direction-based error indicators
  - Enables error capturing for complex supersonic flows
  - Allows for one small nonlinear system solve per adaptation direction
- Adaptation methodology enables factor of two reduction in computational resources for the same level of sonic boom prediction accuracy

Acknowledgments

- This work was partially supported by NASA's Aeronautics Research Mission Directorate (ARMD) Commercial Supersonic Technologies (CST) and Transformational Tools and Technologies (TTT) projects.

- Gratitude is expressed to Brandon Lowe for the development of the LAVA adjoint solver.

- The exceptional contributions of the LAVA team are acknowledged, particularly Scott Neuhoff, James Jensen, James Koch, and Emre Sozer.

- Special thanks are due to Marian Nemec from NASA Ames Research Center for his technical guidance.

- A special thank you to Gaetan Kenway for his supervision of the code development and Cetin Kiris for his exceptional leadership and technical guidance.

- Results in this presentation are from the doctoral dissertation of the first author to be submitted in partial fulfillment of the requirements for a PhD at the University of Kentucky. Special thanks to Peter Hislop and Christoph Brehm for their academic advisory roles.

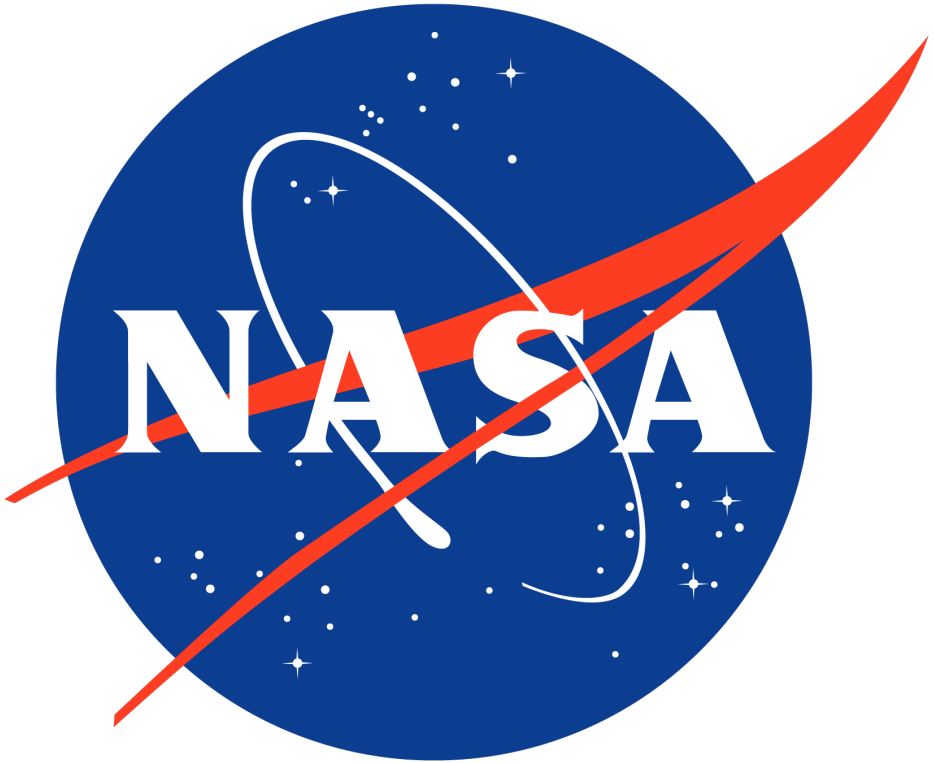
NASA

Results

- A benchmark indicator is formed by propagating uniform coarse and fine CFD solutions to the mid-field

- Pointwise error is computed along the propagated waveform

$$\varepsilon_i = \left| \frac{p_{\mathrm{h},i} - p_{\mathrm{H},i}}{p_\infty} \right|$$

- Mapped to the off-body CFD grid using normalized distance metric

Results: JAXA Wing Body

Reference length : $L_{ref} = 38.7\ m$

Cruise Altitude : 15,276 m

Mach = 1.6, Re/m = 5.7 million, and $\alpha = 2.3^{\circ}$

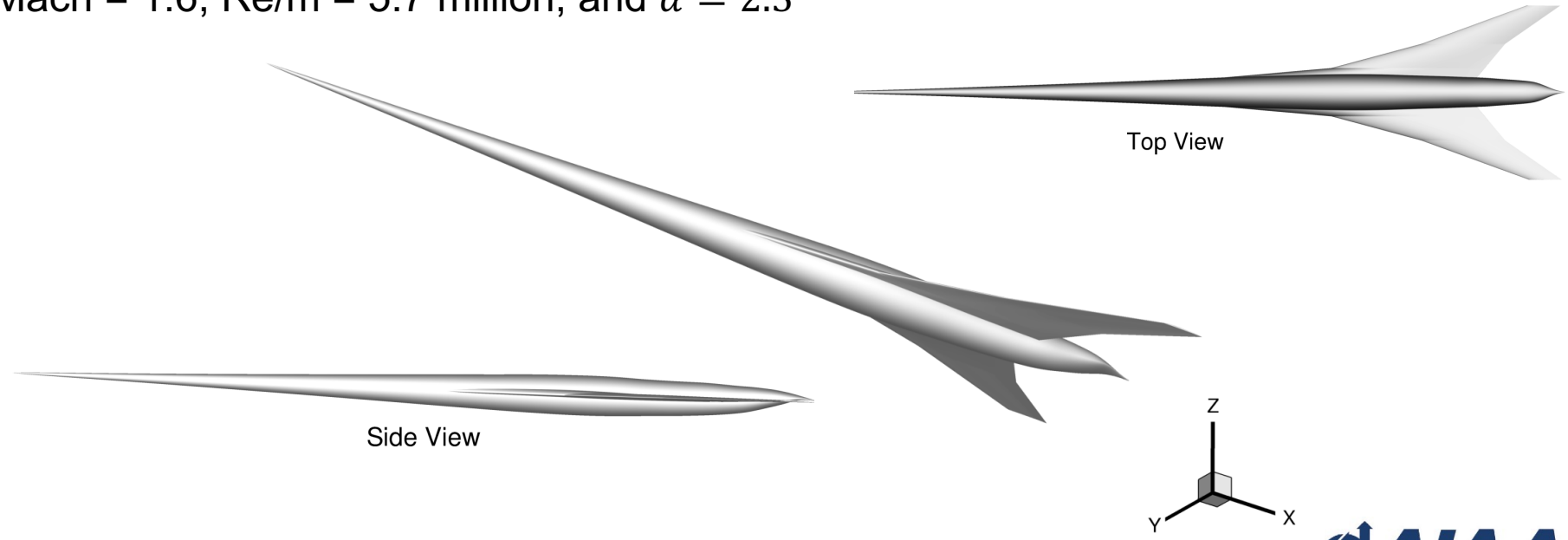

Adjoint Grid Adaptation: Ground-Level Signatures

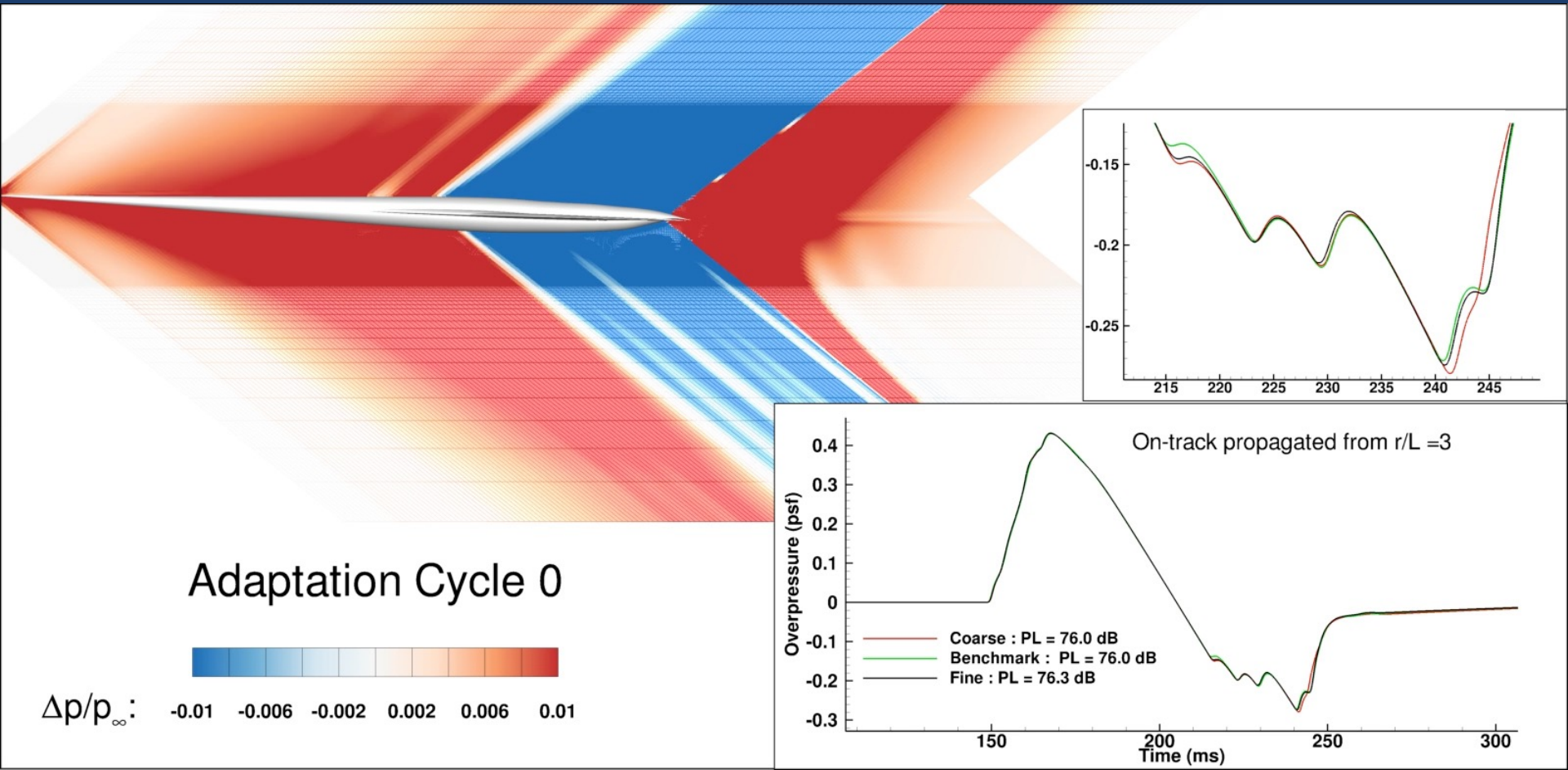

Near-field Accuracy Improvement

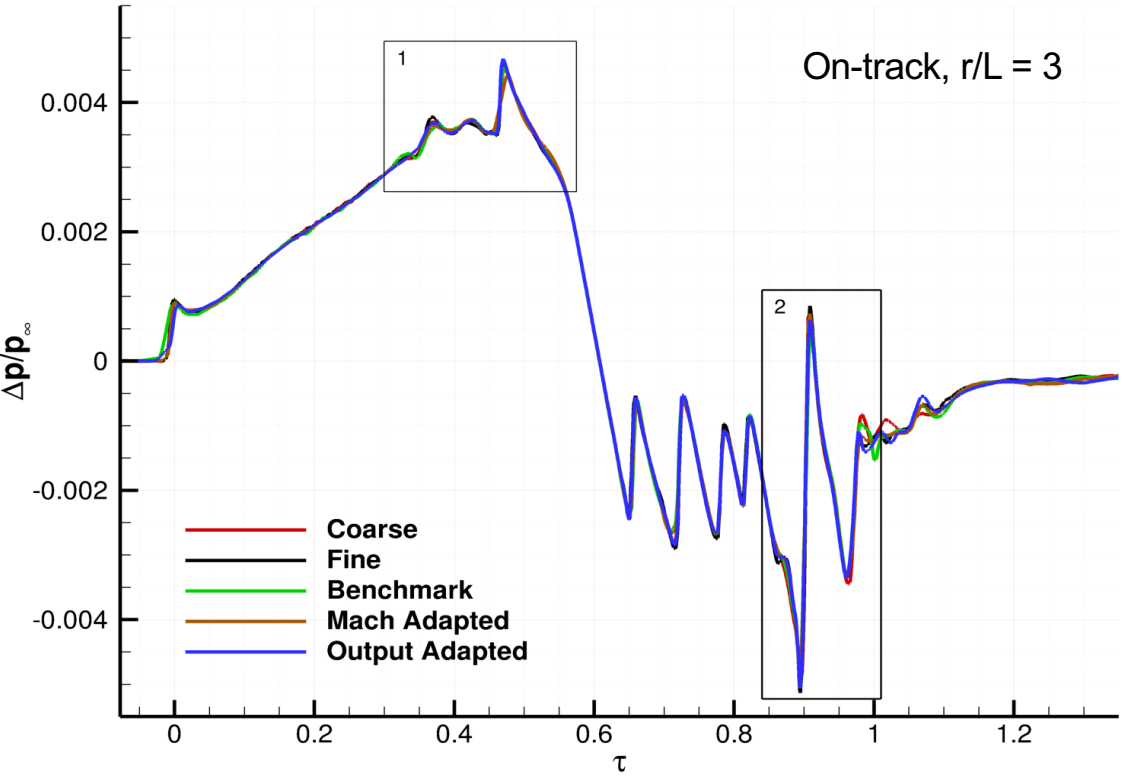

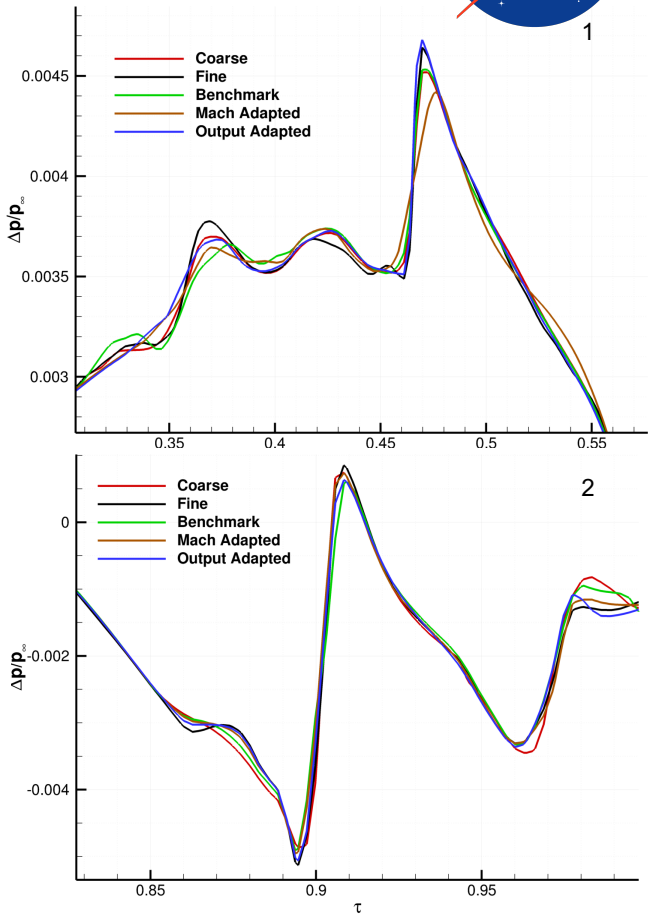

Ground Level Accuracy Improvement

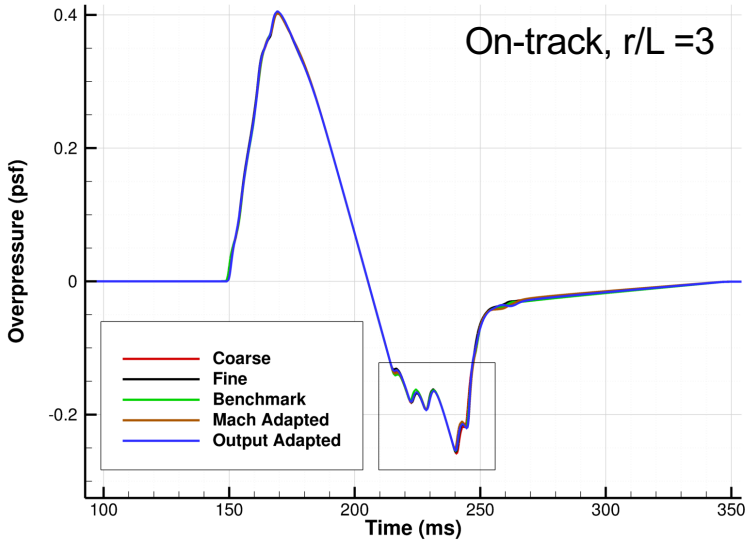

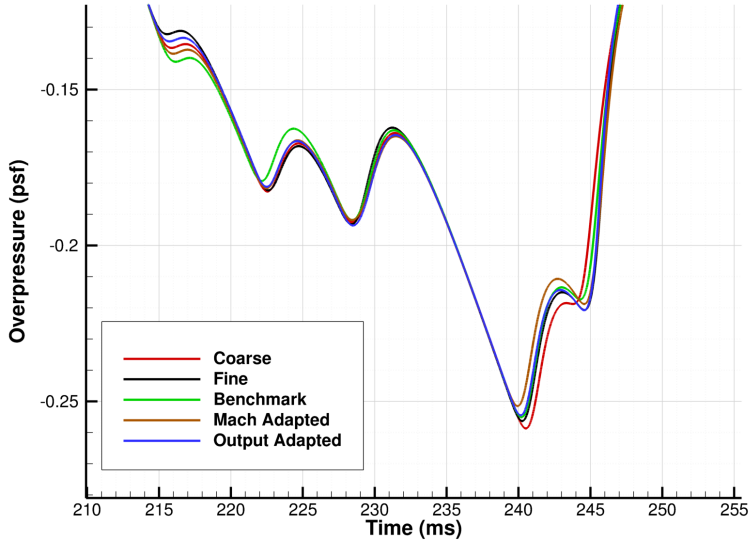

Grid	ASEL [dB(A)]	BSEL [dB]	CSEL [dB(C)]	PL [dB]	ASEL Rel. Error	BSEL Rel. Error	CSEL Rel. Error	PL Rel. Error
Fine	62.15	75.96	90.78	75.98	-	-	-	-
Coarse	60.86	75.43	90.71	74.83	2.064%	0.692%	0.072%	1.514%
Benchmark	61.51	75.45	90.66	75.18	1.026%	0.673%	0.131%	1.045%
Mach Adapted	61.73	75.61	90.66	75.45	0.661%	0.457%	0.134%	0.699%
Output Adapted	62.37	75.86	90.74	76.10	**0.359%**	**0.132%**	**0.048%**	**0.161%**

Cost Analysis

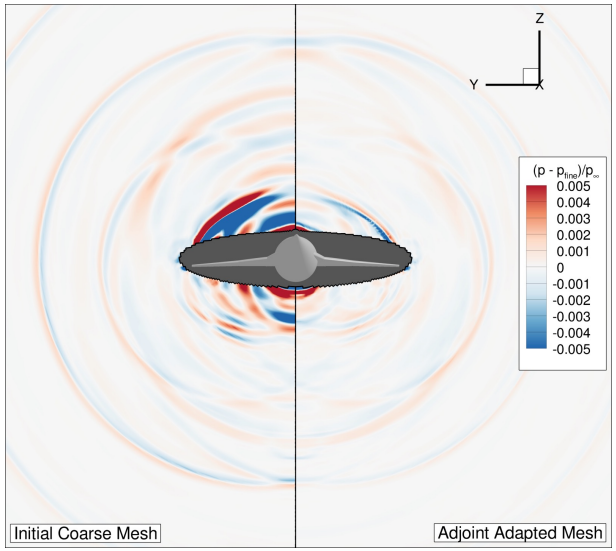

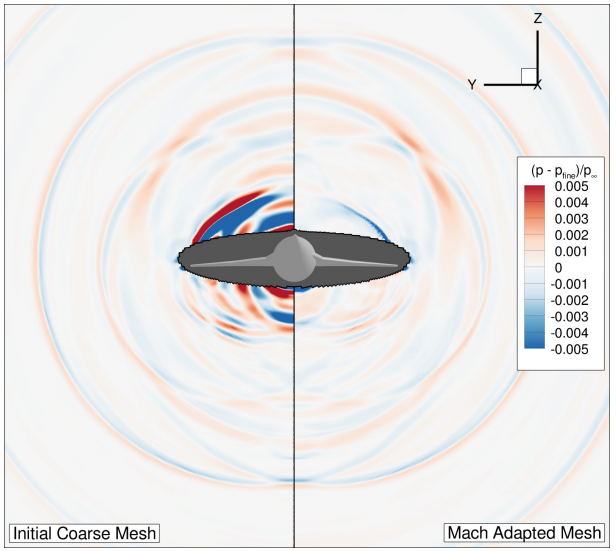

Grid	Connectivity	Primal Solve	Adjoint Solve	Embedding	Adaptation	Restart	**Total**
Coarse	0.14	25.46	-	-	-	-	**25.60**
Benchmark Adapted	0.28	25.46	-	-	0.02	4.70	**30.46**
Mach Adapted	0.29	25.46	-	-	0.01	5.66	**31.42**
Output Adapted	0.28	25.46	0.87	0.17	0.03	5.03	**31.56**
Fine	0.13	55.99	-	-	-	-	**56.12**

Resource usage in CPU-hours for each JWB simulation performed on NASA's Electra supercomputer using 5 Skylake nodes each containing two 20-core Xeon Gold 6148 sockets (2.4 GHz).